Cerebral Cortex, 2020;00: 1–16

doi: 10.1093/cercor/bhaa064
Original Article

ORIGINAL ARTICLE

TRIM32 Deficiency Impairs Synaptic Plasticity by Excitatory-Inhibitory Imbalance via Notch Pathway

Michael Ntim[1], Qi-Fa Li[1], Yue Zhang[1], Xiao-Da Liu[1], Na Li[2], Hai-Lun Sun[1], Xuan Zhang[2], Bakhtawar Khan[1], Bin Wang[1], Qiong Wu[1], Xue-Fei Wu[1], Williams Walana[3], Khizar Khan[1], Quan-Hong Ma[4], Jie Zhao[2] and Shao Li[1]

[1]Liaoning Provincial Key Laboratory of Cerebral Diseases, Department of Physiology, College of Basic Medical Sciences, Dalian Medical University, Dalian, China, [2]National-Local Joint Engineering Research Center for Drug-Research and Development (R & D) of Neurodegenerative Diseases, Dalian Medical University, Dalian, China, [3]Department of Immunology, College of Basic Medical Sciences, Dalian Medical University, Dalian, China and [4]Institute of Neuroscience and Jiangsu Key Laboratory of Neuropsychiatric Diseases, Soochow University, Suzhou, China

Address correspondence to Shao Li, Liaoning Provincial Key Laboratory of Cerebral Diseases, College of Basic Medical Sciences, Dalian Medical University, No 9 Western Section, Lvshun South Road, Dalian City, P.R. China 116044. Email: lishao89@dmu.edu.cn; Jie Zhao, National-Local Joint Engineering Research Center for Drug-Research and Development (R & D) of Neurodegenerative Diseases, Dalian Medical University, No 9 Western Section, Lvshun South Road, Dalian City, Dalian City, P.R. China 116044. Email: dlzhaoj@163.com; Quan-Hong Ma, Institute of Neuroscience and Jiangsu Key Laboratory of Neuropsychiatric Diseases, Soochow University, Dushuhu campus of Soochow University, 199 Ren-Ai Road, Suzhou, Jiangsu, P.R. China 215123. Email: maquanhong@suda.edu.cn.
Michael Ntim, Qi-Fa Li, Yue Zhang authors have contributed equally to this work

Abstract

Synaptic plasticity is the neural basis of physiological processes involved in learning and memory. Tripartite motif-containing 32 (TRIM32) has been found to play many important roles in the brain such as neural stem cell proliferation, neurogenesis, inhibition of nerve proliferation, and apoptosis. TRIM32 has been linked to several nervous system diseases including autism spectrum disorder, depression, anxiety, and Alzheimer's disease. However, the role of TRIM32 in regulating the mechanism of synaptic plasticity is still unknown. Our electrophysiological studies using hippocampal slices revealed that long-term potentiation of CA1 synapses was impaired in TRIM32 deficient (KO) mice. Further research found that dendritic spines density, AMPA receptors, and synaptic plasticity-related proteins were also reduced. NMDA receptors were upregulated whereas GABA receptors were downregulated in TRIM32 deficient mice, explaining the imbalance in excitatory and inhibitory neurotransmission. This caused overexcitation leading to decreased neuronal numbers in the hippocampus and cortex. In summary, this study provides this maiden evidence on the synaptic plasticity changes of TRIM32 deficiency in the brain and proposes that TRIM32 relates the notch signaling pathway and its related mechanisms contribute to this deficit.

Key words: excitatory-inhibitory imbalance, notch, synaptic plasticity, TRIM32

Introduction

Tripartite motif-containing protein 32 (TRIM32) is a member of the tripartite motif protein family, a neural stem cell (NSC) inhibitory protein as well as a transcription factor. Reports show that TRIM32 possesses an E3 ubiquitin ligase activity (Liu et al. 2014). The presence of a RING domain gives most members of

the TRIM family and their E3 ligase activity, and this makes them undergo ubiquitination of specific substrates, one of how they exert their biological functions (Meroni and Diez-Roux 2005). Physiologically, E3 ubiquitin ligases control homeostasis, cell cycle, as well as several DNA repair pathways. The E3 ubiquitin ligases are engaged mainly in modifying their targets posttranslationally through a myriad of ubiquitin-modifying reactions which eventually produces a conjugation of a ubiquitin moiety onto a target substrate (Pickart and Eddins 2004). Nicklas et al. observed that TRIM32 initiates the differentiation of neurons and self-renewal is suppressed by the ubiquitination of the c-Myc transcription factor and certain microRNAs activation (Nicklas et al. 2012). TRIM32 protein was reported to be almost absent in NSCs both in the SVZ and in the DG. The NSCs that are found in the inner zone of the DG show higher nuclear expression of TRIM32 as soon as they become neuroblasts or immature neurons and come to the outer layer of the DG. This is an indication that TRIM32 is upregulated upon differentiation of the NSC (Hillje et al. 2015).

TRIM32 plays other important roles including neurogenesis, inhibition of nerve cell proliferation, and restriction of apoptosis (Hillje et al. 2013). Many abnormalities in some protein expressions in the brain have been linked to TRIM32 overexpression or downregulation. There has been a strong association between TRIM32 regulation and the development of certain neurological disorders such as depression (Snyder et al. 2011), anxiety (Lionel et al. 2013), Alzheimer's Disease (Yokota et al. 2006), autism spectrum disorder (ASD) (Ruan et al. 2014), and attention deficit hyperactivity disorder (ADHD) (Lionel et al. 2011). Many of these neurological disorders have been suggested by numerous studies to have synaptic plasticity deficits as one of their resultant outcomes. Though there has not been a direct study on the effect of TRIM32 deficiency on synaptic plasticity, it has been speculated that the absence of TRIM32 does alter synaptic plasticity because of its links to these neurological disorders.

With the numerous research advances on the functions of TRIM32, it remains unclear the effect of TRIM32 on synaptic plasticity. We, therefore, proposed that TRIM32 could influence changes in synaptic plasticity. Using the TRIM32 knockout (KO) mice model, we studied long-term potentiation (LTP) using electrophysiology, various staining techniques, and western blotting to ascertain receptor expressions and neuron numbers as well as electroencephalogram (EEG) to establish that TRIM32 deficiency impairs synaptic plasticity and leads to increase in the notch and its related pathway elements. This study also provides the maiden evidence that TRIM32 relates to the notch signaling pathway and reports that an inhibition of notch could rescue synaptic plasticity deficits in vitro.

Experimental Methods

Experimental Animals

TRIM32 KO (TRIM32$^{-/-}$) mice of reproductive ages were given to us by Prof. Melitta Schachner from Universität Hamburg, Germany and bred in the Specific Pathogen Free (SPF) Model Animal Center of Dalian Medical University, China. Adult mice (male and female) were housed in groups with the temperature-controlled at 25 °C, with an adequate supply of feed and water. Animals had a 12-h day light and night cycle. TRIM32 KO mice and their wild-type (WT) littermate (control) were raised in the same conditions and were used for the experiments. All animal experiments were carried out following the Institutional Animal Care and Use Committee guidelines of NIH, USA (NIH publication no. 86–23, revised 1987) and approved by the Institutional Ethics Committee of the Dalian Medical University.

Genotyping of TRIM32 Mice

The genotype of TRIM32 mice was confirmed before the animals were used for the various experiments. Genotyping was done using the following primer sequences:

TRIM32 WT1 (5′-3′): GGAGAGACACTATTTCCTAAGTCA

TRIM32 WT2 (5′-3′): GTTCAGGTGAGAAGCTGCTGCA

TRIM32 Mu (5′-3′): GGGACAGGATAAGTATGACATCA

The primer-pairs WT1 and WT2, as well as WT1 and Mu, were used to determine WT and knockout mice, respectively. The PCR reaction conditions were set at 95 °C (5 min) for enzyme activation, 40 cycles of denaturation at 95 °C for 30 s, annealing at 55 °C for 35 s, extension at 72 °C for 60 s, then 72 °C for 5 min, and finally at 4 °C infinitely. The amplified DNA was separated on a 2% agarose gel by electrophoresis using a current of 120 mA for 60 min. WT and knockout bands were detected at 250 and 300 bp, respectively, compared with the standard DNA ladder.

LTP Measurements

Adult TRIM32 KO and WT mice were deeply anesthetized with 4% chloral hydrate intraperitoneal to ease pain and quickly decapitated at the neck. Electrophysiological recordings were carried out as previously described by Li et al. (2019). Stimulation intensity was set to evoke 40–50% of the maximal response of fEPSP amplitudes. LTP was induced using high-frequency stimulation (HFS) (four 100 Hz and 1-s trains delivered 20 s apart).

Input–Output Curves Analysis

Input–output (I/O) experiments were established by single-pulse stimulation of the Schaffer collaterals region to evaluate synaptic potency by increasing the stimulus current intensity by steps of 0.1 mA (0.05–1.0 mA). This was done to examine whether the properties of basic synaptic transmission at Schaffer collateral-CA1 synapses are altered. Stimulus pulses were delivered at a frequency of 0.033 Hz, and five responses at each current intensity were averaged.

Paired-Pulse Facilitation Analysis

Paired-pulse facilitation (PPF), presynaptic facilitation, was conducted immediately after the I/O tests using a frequency of 0.033 Hz. Pairs of identical stimuli were delivered in closely spaced interstimulus intervals of 25, 50, 75, 100, 125, 150, and 200 ms, and the average value of five independent recordings in each interval was used. Facilitation was measured as a ratio of the second pulse-evoked EPSP slope to the first evoked. The data were acquired with an Axon multiclamp 700 B amplifier, filtered at 10 000 kHz, digitized at 10 kHz, and analyzed offline using pClamp10.3 software (Molecular Devices Corp.).

Nissl Staining

Brains of 12-week-old mice were harvested and sectioned as described above and mounted on charged glass slides, rehydrated, and stained with 0.1% Cresyl violet dye (Sigma). The

slides were dehydrated with 70%, 90%, 100% ethanol, and xylene and mounted with a cover glass. Images were taken with a Panoramic fluorescence scanner (3DHISTECH Ltd.). The number of stained neurons was estimated per unit square area using ImageJ software (NIH). Images were captured from different sections of the stained tissues, and at least, three images from each group were used for the analysis.

Golgi Staining and Analysis

Adult TRIM32 KO mice and WT littermate control mice were anesthetized with 4% chloral hydrate intraperitoneal and rapidly decapitated. One brain hemisphere was used for Golgi staining. The brains were incubated in Golgi solution A + B for 14 days (FD Rapid GolgiStain Kit; FD NeuroTechnologies) according to the manufacturer's protocol. The brains were sliced using a Vibratome (VT1200S; Leica) at a thickness of 200 µm and mounted on glass slides coated with 3% gelatin. The sections were air-dried for 24 h in the dark at room temperature. Staining procedures were followed as described in the manufacturer's protocols. Dendritic images were taken from CA1 pyramidal neurons by microscope under bright-field using a Panoramic fluorescence scanner (3DHISTECH Ltd.). Dendritic spines were then counted in a blinded manner using ImageJ software (NIH). Further analysis of spine number and morphological characteristics was done using Reconstruct software as described by Risher et al. (2014).

Primary Neuron Culture and Inhibitor Treatments

Primary neurons were prepared from brains of 1-day-old C57 mice (SPF of Dalian Medical University). Briefly, mice were quickly decapitated after freezing with an ice pack to cause minimum pain. The meninges were removed, the cortex and hippocampus were mechanically dissected and digested with 0.125% trypsin in DMEM medium cell culture incubator for 20 min, and then the cell suspension was centrifuged at 1500 rpm for 5 min. The supernatant was discarded, and the cell aggregation was resolved to a single-cell suspension. Primary neurons were plated into a 24-well culture plate (NEST Biotechnology) with 10% FBS-DMEM (Neurons plant medium) after 4 h replaced 10% FBS-DMEM with neurons maintenance medium which contains 95% Neurobasal, 2% B27, 1% penicillin/streptomycin, 1% L-glutamine (ThermoFisher scientific). Cells were cultured at 5% CO_2, 37 °C and half of the medium changed every 2 days. A gamma-secretase inhibitor, DAPT (Macklin), was dissolved in DMSO and administered at a concentration of 1, 5, and 10 µM with an equal concentration of DMSO administered every other day. Protein and RNA were harvested on the 12th day.

Quantitative Real-Time Polymerase Chain Reaction

Total RNA was isolated from the hippocampus with Trizol reagent (ThermoFisher Scientific) according to the manufacturer's protocol. Complementary DNA (cDNA) was synthesized from 1 µg total RNA using the first-strand cDNA synthesis kit (TransGen Biotech). The expression levels of targeted genes in three or four cohort littermates of mice were performed using the TransStart Top Green qPCR SuperMix (TransGen Biotech) on CFX96 real-time system (BIO-RAD). Threshold cycle (CT) values for the genes were calculated, and changes were assessed using the formula $2^{-\Delta\Delta CT}$, where ΔCT represents the difference in CT values between the target and housekeeping gene (GAPDH) mRNA. The forward and reverse primer sequences used are listed below

NR1 5′ -AGTGGAACGGAATGATGGGAG - 3′

5′ -CCGAACCCATGTCTTATCCAG - 3′

NR2A 5′ -AGCCCCCTTCGTCATCGTAGA - 3′

5′ -ACCCCTTGCAGCACTTCTTCAC - 3′

NR2B 5′ -GCCATGAACGAGACTGACCC - 3′

5′ -GCTTCCTGGTCCGTGTCATC - 3′

GluA1 5′ -GAGCAACGAAAGCCCTGTGA - 3′

5′ -CCCTTGGGTGTCGCAATG - 3′

$GABA_A$ 5′-GCATGTATGTCTGCAGGA- 3′

5′-CTGACACCTACTTCCTGA- 3′

PSD95 5′ -TGAGATCAGTCATAGCAGCTACT-3′

5′ -CTTCCTCCCCTAGCAGGTCC - 3′

SYP 5′ -CAGTTCCGGGTGGTCAAGG - 3′

5′ -ACTCTCCGTCTTGTTGGCAC - 3′

SYN1 5′ -AGCTCAACA AATCCCAGTCTCT- 3′

5′ -CGGATGGTCTCAGCTTTCAC -3′

NGF 5′ -GCCCACTGGACTAAACTTCAGC - 3′

5′ -CCGTGGCTGTGGTCTTATCTC - 3′

NGN3 5′ -CAATCGAATGCACAACCTCA - 3′

5′ -GGGAGACTGGGGAGTAGAGG - 3′

HES1 5′ -GACGGCCAATTTGCCTTTCTCATC-3′

5′ -TCAGTTCCGCCACGGTCTCCACA -3′

Notch1 5′ -GCTACAACTGCGTGTGTGTC - 3′

5′ -GTTGGTGTCGCAGTTGGAGC - 3′

Mash1 5′ -AGGCCCTACTGGGAATGGA- 3′

5′ -CCCTGTTGCTGAGAACATTGA - 3′

GAPDH 5′ -CACTGGCATGGCCTTCCGT - 3′

5′ -CTTACTCCTTGGAGGCCAT - 3′

Western Blotting

Western blotting was carried out as previously reported by Wang et al. (2019). The primary antibodies used were GluA1 (1: 1000, Abcam ab31232), $GABA_A$ (1:1000, Abcam ab10098), NR1 (1:500, BD Pharmingen 556 308), NR2A (1:500, Millipore MAB5216), NR2B (1:1000, Abcam ab93610), Synaptophysin (1:1000, Millipore MAB5258), GAP-43 (1:1000, Millipore MAB5220), PSD95 (1:1000, Abcam ab2723), Synapsin 1 (1:1000, Abcam ab64581), Notch1

(1:1000, Abcam ab8925), Hes1 (1:1000, Abcam ab108937), Neurogenin3 (1:1000, Abcam ab176124), NGF (1:1000, Abcam ab52918), EAAT2 (1:1000, Millipore MAB2262), SLC32A1 (1:1000, Abcam ab42939), and β-actin (1:2000, Abcam ab8227). The membranes were incubated with the appropriate species-specific HRP-conjugated secondary antibody (15 000, Thermofisher). The bands were detected using enhanced chemiluminescence (ECL, Thermofisher). A ChemiDoc MP imaging system (BioRad) was used to capture images, and protein bands were quantified and analyzed with ImageJ software (NIH).

Immunohistochemistry

Immunostaining was conducted as previously reported by Wang et al. (2019). Primary antibodies applied were: GluA1 (1:200, Abcam ab31232), $GABA_A$ (1:200, Abcam ab10098), NR1 (1:500, BD Pharmingen 556 308), NR2B (1:1000, Abcam ab93610), SLC32A1 (1:200, Abcam), and EAAT2 (1:200, Millipore). Slices were incubated in Alexa Fluor conjugated secondary antibody (1:500, Invitrogen). DAPI staining followed. The slices were imaged with a Panoramic fluorescence scanner (3DHISTECH Ltd, Hungary). Mean fluorescence intensities were determined blindly using ImageJ software (NIH).

Surgery and Electrophysiological Neural Data acquisition

TRIM32 WT and KO transgenic mice (10–12 weeks old) were acutely anesthetized with volatilized isoflurane to keep mice alive during the period of recording. The mouse was quickly fixed on stereotaxic apparatus (David Kopf Instruments, Model 902) and mounted with a mask that supplied 2.5% of volatilized Isoflurane throughout the surgery and recording time. Tail or toe pinching was done before the surgery to inspect the depth of anesthesia. The scalp was incised on the midline about 10 mm to expose the skull. Any debris on the skull was wiped off with saline-soaked cotton tips. The bregma and lambda points were marked and set in the same horizontal plane. Three screws were placed in the skull (two frontal areas and one parietal area) to touch the dura mater over the surface of the cortex. An area of the skull (about 2 mm $\times$ 2 mm) on the other parietal area was also removed to receive the recording electrodes. The blood-brain barrier was carefully removed to enable the electrodes to have access to the brain. The multichannel recording electrode was directed to that area and lowered to penetrate the cortex at about 500 µm from the surface of the cortex using the stereotaxic apparatus.

Neural signals were recorded in a wide frequency band (0.01–40 000 Hz) and amplified 1000–2000 times before digitization using Plexon Recorder System (Plexon) under isoflurane-induced anesthetic conditions.

Sorting and Analysis of Neural Data

Neural data recorded were sorted into unit(s) (usually 1–2 units/channel) using Offline Sorter software (version 4.1.0, Plexon Inc). All the recordings per animal were autosorted with a batched command file for consistency. A threshold of -5 sigmas from the mean was used during the sorting. Manual checking was then performed to ensure that spike waveforms were consistent and that the cluster boundaries were distinct. All isolated units showed recognizable refractory periods (>1 ms) in the interspike histograms. The units that were included in the analysis had an L-ratio less than 0.5 and an isolated distance greater than 15. Using NeuroExplorer (version 5.030, Nex Technologies), the spike frequency per animal using instant frequency analysis was obtained and the mean spike frequencies were computed per group. To obtain the spectral power for the various bandwidth, the spectrogram analysis was performed.

Statistical Analysis

All statistical analyses were performed using GraphPad Prism 7 (GraphPad Software), and data are presented as mean $\pm$ SEM. Unpaired *t*-test was used to analyze differences between two groups, and one-way ANOVA was used to analyze more than two groups (Turkey's post hoc analysis was used to compare differences). *P*-value < 0.05 was considered statistically significant for all analyses.

Results

LTP Is Impaired and Dendritic Spine Characteristics Altered in TRIM32-Deficient Mice

To investigate the effect of TRIM32 on synaptic plasticity, we used electrophysiology techniques to record the LTP of TRIM32 KO mice and their WT littermates. The changes in hippocampal synaptic plasticity (functional) were inferred from the LTP recording. LTP recordings indicated changes in fEPSPs slope before and after HFS in different groups of mice (Fig. 1A[*a*]). The slope and peak amplitude of the EPSP in the WT mice were significantly higher than those of the TRIM32 KO mice: slope (173.8% $\pm$ 7.285% vs. 149.5% $\pm$ 6.44%) and amplitude (179.7% $\pm$ 10.98% vs. 148.8% $\pm$ 8.675%) in WT and KO mice, respectively (Fig. 1A[*b*, *c*], $P < 0.05$). The properties of basic synaptic transmission at Schaffer collateral-CA1 synapses were examined. I/O curves were analyzed by measuring the postsynaptic potential slope with various stimulus intensities (0.05–1.0 mA) before the induction of LTP. Data were normalized with 100% as the highest amplitude (an average of five sweeps were selected at each of the stimulation intensities) of fEPSP. TRIM32 KO mice showed no significant change in the I/O curve compared with WT littermates (Fig. 1A[*d*]), suggesting that the absence of TRIM32 does not directly affect the basal synaptic response. PPF was recorded after the I/O curve to determine the probability of synaptic vesicle (SV) release at intervals between 0 and 250 ms. As shown in Figure 1A(*e*), the obtained PPF recordings showed no significant difference in the short-term synaptic plasticity between TRIM32 KO mice and their WT littermates. However, a slight decrease in the PPF ratio in the KO mice was observed (Fig. 1A[*e*]).

A recent report has shown the relationship between LTP (functional plasticity) and dendritic spines (structural plasticity) (Kasai et al. 2010). Changes in dendritic spine densities were quantified at the pyramidal neurons in the hippocampal CA1 areas. Herein, a difference in dendritic spine morphology and density was observed. The spine density was reduced in the TRIM32 KO group in CA1 and CA3 (Fig. 1B[*b*, *c*], $P < 0.05$). The percentage of mushroom-type spines was lower in the TRIM32 KO mice group in the CA1 and CA3 regions (Fig. 1B[*d*]). Stubbiness of the spines was done using length to width ratio (LWR) < 1. Herein, TRIM32 KO showed an increased percentage of stubby spines (Table 1). Our results indicate that the average LWR was significantly reduced in TRIM32KO in CA1 and CA3 (Fig. 1B[*e*]). Likewise, the average protrusion from the dendrite was decreased in TRIM32 KO mice with significance in the

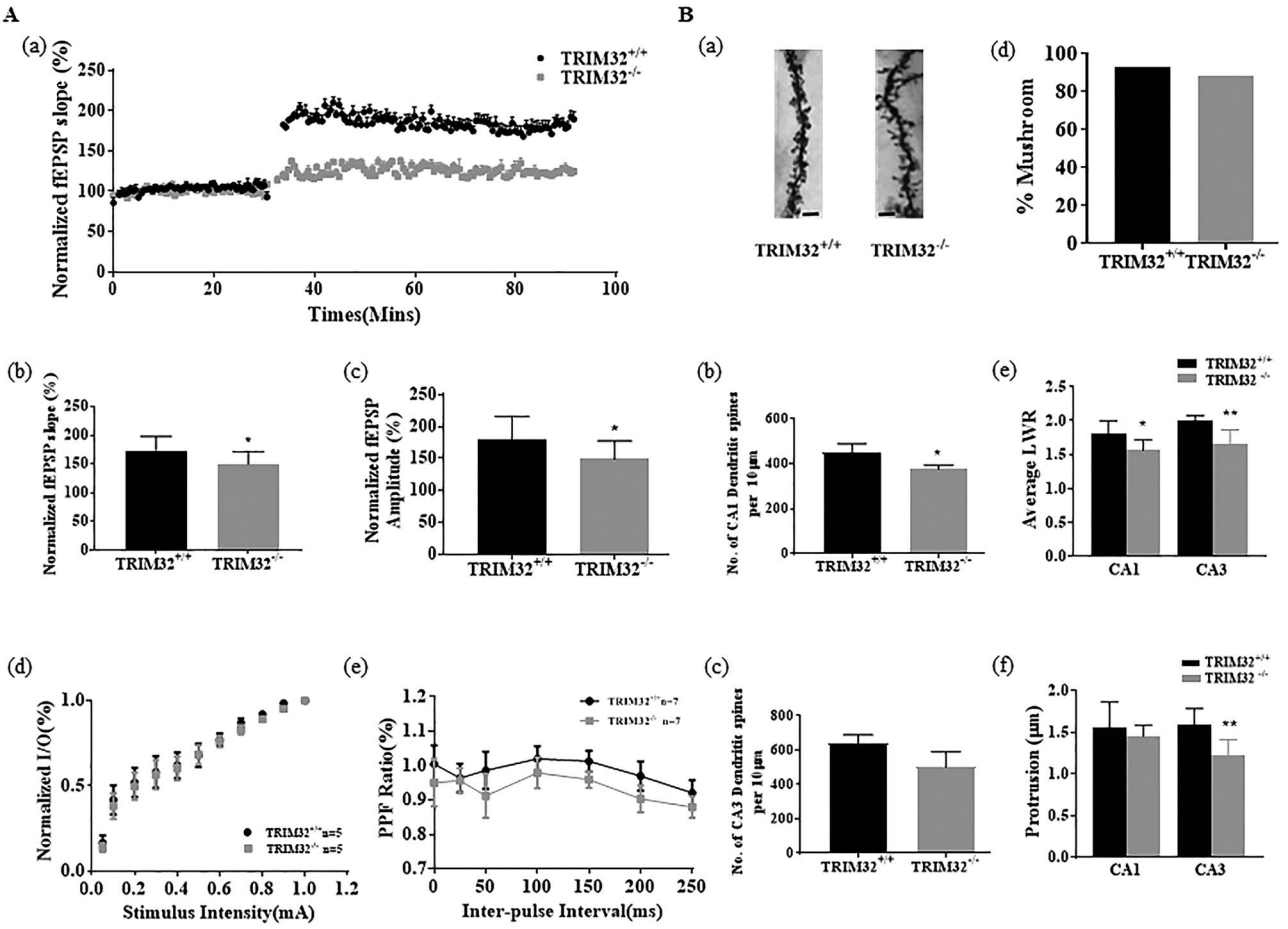

Figure 1. Synaptic plasticity is altered in TRIM32 KO mice. (*A*) Functional plasticity is altered in TRIM32 KO mice even though basic synaptic transmission is not altered (*a*) Time course of the effects of HFS on the fEPSP initial slope. (*b* and c) Cumulative data showing mean fEPSP peak amplitude and mean fEPSP slope 60 min post-HFS. (*d*) I/O plots of fEPSP slopes versus current input (µA) were similar in WT and TRIM32 KO mice ($n = 5$ mice in each group), indicating lack of TRIM32 did not alter baseline synaptic transmission. (*e*) PPF analysis showing the S1/S2 ratios for increasing stimulation interpulse intervals in slices from WT and TRIM32 KO mice ($n = 7$ mice in each group). (*B*) Structural plasticity is altered in TRIM32 KO mice. (*a*) Representative micrographs of dendritic spines in TRIM32 KO and WT mice (Scale bar: 10 µm). (*b*) Bar graph showing CA1 pyramidal cell dendritic spine density in TRIM32 KO mice and WT littermates. (*c*) Bar graph showing CA3 pyramidal cell dendritic spine density in TRIM32 KO and WT mice. (*d–f*) Bar graphs showing the percentage of mushroom-type spines (*d*), average LWR (*e*) and length of protrusions (*f*) in CA1and CA3 in TRIM32 KO and WT mice. Data were expressed as means ± SEM. $^{*}P < 0.05$, $^{**}P < 0.01$.

CA3 region. A greater percentage of the dendritic spines were thinner at the stem and smaller in the head compared with their WT littermates having a bulge-headed spine and thicker stems (Fig. 1B[a], Table 1).

TRIM32 Deficiency Showed Decreased Synaptic Plasticity Proteins

Synaptophysin, Synapsin1, Growth-associated protein-43 (GAP-43) and Postsynaptic density-95 (PSD-95) genes are critical for effective synaptic function and were analyzed for their expression at the mRNA and protein levels. Considering Synaptophysin, Synapsin1, and GAP-43 at the presynaptic side and PSD-95 for the postsynaptic side, significant decreases in protein expression levels for SYP, GAP-43, SYN1(Fig. 2A[a,b], $P < 0.05$, 0.01), and PSD-95 (Fig. 2B[a,b], $P < 0.05$) were observed in TRIM32 KO mice. Similarly, a significant decrease in psd95 mRNA (Fig. 2B[c], $P < 0.05$) and a marginal decrease in syp and syn1 mRNA (Fig. 2A[c]) were observed in TRIM32 KO mice. These data suggest that TRIM32 KO impair synaptic plasticity by downregulating these synaptic proteins. AMPA receptors (AMPARs) are important mediators for synaptic plasticity. AMPAR protein expression was declined in TRIM32 KO mice (Fig. 2C[a,b], $P < 0.01$). Treating coronal sections of brain slides stained with antibodies reactive against AMPARs confirmed this result (Fig. 2C[c]).

TRIM32 Deficiency Leads to Decreased GABA and Increased NMDA Receptor Expression Resulting in an Imbalance in Excitation and Inhibition

Examining the potential mechanism underlying the impairment of synaptic plasticity in TRIM32 KO mice, enormous reports on the important roles of the balance of GABA and NMDA play in synaptic plasticity could not be overlooked. Hence, these receptors' expressions were investigated. $GABA_A$ protein expression was significantly reduced in TRIM32 KO by western blot analysis (Fig. 3A[*a*, *b*], $P < 0.05$). Staining brain slides with antibody immunoreactive against $GABA_A$ receptors confirmed the above (Fig. 3A[c]). Messenger RNA (mRNA) expressions of NR1 and

Table 1 Characteristics of dendritic spines in CA1 and CA3 regions of TRIM32 KO and WT mice

Morphology/Characteristics	CA1		CA3	
	$TRIM32^{+/+}$ ($n = 218$)	$TRIM32^{-/-}$ ($n = 180$)	$TRIM32^{+/+}$ ($n = 140$)	$TRIM32^{-/-}$ ($n = 117$)
Mushroom (width > 0.6 μm)	203 (93.11%)	159 (88.3%)	128 (91.4%)	96 (82.1%)
Filopodia (length > 2 μm)	55 (25.2%)	25 (13.9%)	34 (24.3%)	11 (9.4%)
Stubby (LWR < 1)	41 (18.8%)	44 (24.4%)	8 (5.7%)	19 (16.2%)
Long thin (length < 1 μm)	64 (29.4%)	43 (23.9%)	29 (20.7%)	46 (39.3%)
Thin (length < 2 μm)	162 (70.6%)	154 (85.6%)	106 (75.7%)	106 (90.6%)
Branches (2 or more)	15 (6.9%)	5 (2.8%)	9 (6.4%)	4 (3.4%)

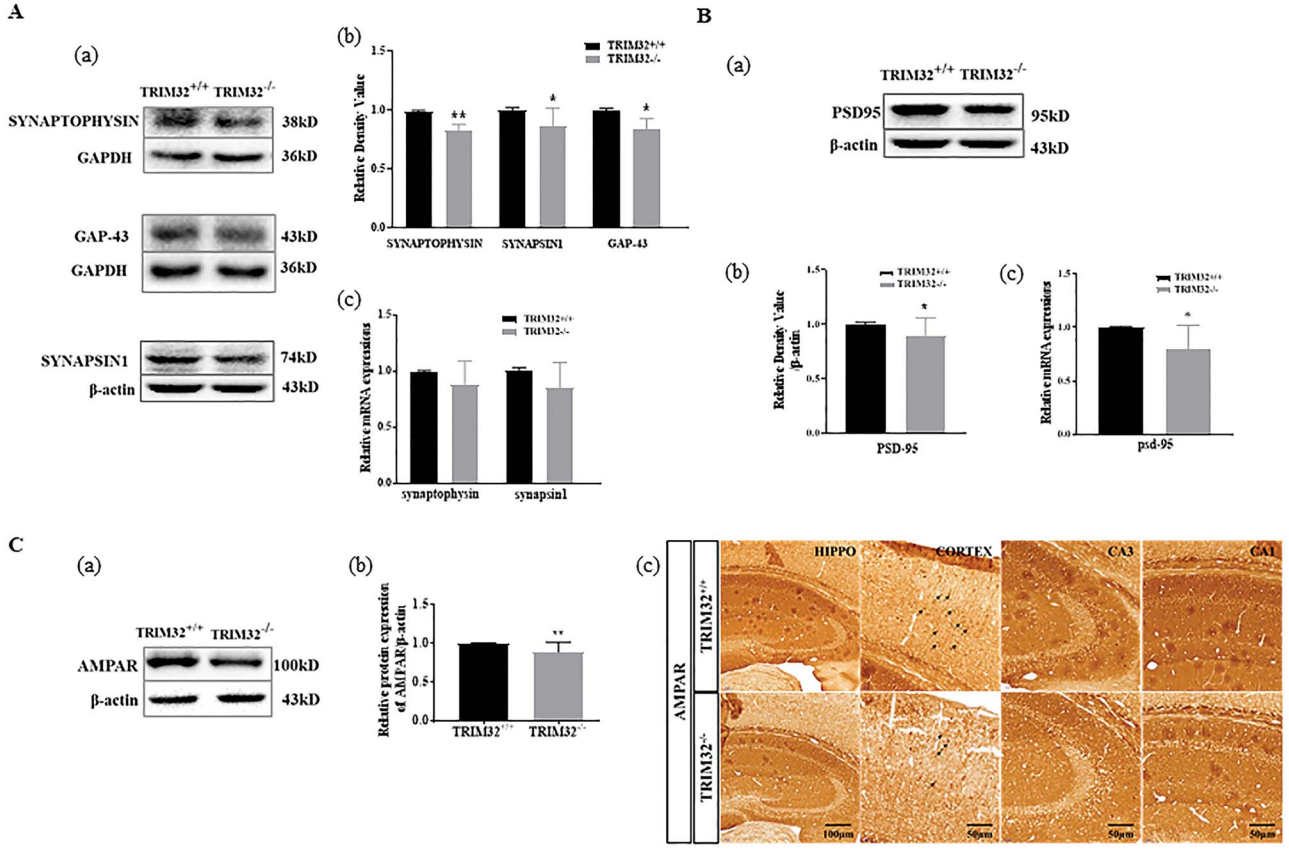

Figure 2. TRIM32 KO changes synaptic plasticity proteins. (*A*) Presynaptic proteins reduced in the hippocampal brain lysates of TRIM32 KO mice. (*a*) Representative immunoblots (*b*) and densitometry analyses showing Synaptophysin, Synapsin1, and GAP-43 expressions (*c*) Relative mRNA expression of RT-qPCR showed that expression levels of syp and syn1 decreased in the hippocampus of TRIM32 KO mice. (*B*) Postsynaptic protein (PSD95) was downregulated in hippocampal brain lysates of TRIM32 KO mice. (*a*) Representative immunoblots (*b*) and densitometry analyses showed that PSD-95 is significantly downregulated in the hippocampus of the TRIM32 KO mice. (*c*) Relative mRNA expression of RT-qPCR showed that the expression level of psd95 is significantly downregulated in the hippocampus of TRIM32 KO mice. (*C*) AMPARs were downregulated in TRIM32 KO mice. (*a*) Representative immunoblot and (*b*) densitometry analysis of the immunoblots showed that the expression levels of AMPAR significantly decreased in hippocampal lysates of TRIM32 32 KO mice. (*c*) Coronal sections of the brain were immunohistochemically stained with an antibody against AMPARs. Here, Synaptophysin, Synapsin1, GAP-43, PSD95, AMPAR, and their corresponding β-actin/GAPDH immunoblots were performed on different parts of the PVDF membrane of different gels (obtained from at least 10 brain samples in each group) in the western blotting whereas syp, syn1, and psd95 were normalized to gapdh. Data (means ± SEM) are from at least three independent cohorts of mice littermates with a total of at least 10 mice ($n = 3$). $^{*}P < 0.05$, $^{**}P < 0.01$.

NR2B were marginally increased while NR2A significantly increased in TRIM32 KO mice (Fig. 3B[c], $P < 0.05$). The mRNA increases, commensurate their respective protein expressions (Fig. 3B[*a*, *b*], $P < 0.05$). More so, the expressions of NR1 and NR2B were increased in immunostained coronal sections of brain slides (Fig. 3B[*d*, *e*]). Having established that TRIM32 KO reduced $GABA_A$- and increased NMDA-receptor expressions, the influence in the balance between excitatory and inhibitory transmissions was investigated. Protein expression levels of excitatory amino acid transporter 2 (EAAT2) and SLC32A1 (which are markers for excitatory and inhibitory transporters, respectively) were analyzed by western blotting. A significant upregulation in EAAT2 expression and a downregulated SLC32A1 expression in hippocampal brain lysates were observed

in TRIM32 KO mice (Fig. 3C[*a*, *b*], $P < 0.05, 0.01$). Double immunostaining of the various regions of the hippocampus and cortex for EAAT2 and SLC32A1 expressions confirmed the above results (Fig. 3D[a–h]).

Overexcitation Is Associated with Decrease Neuronal Numbers in TRIM32-Deficient Mice

The occurrence of imbalance in excitatory and inhibitory transmission leads to overexcitation and is usually characterized by an increased spike activity in the brain. EEG recorded and analyzed, showed that the number and frequency of spikes occurring during an estimated period of 4000 s were significantly increased in the TRIM32 KO mice (Fig. 4A[c], $P < 0.05$). The same was also observed in the trace of spike activity recorded (representative in Fig. 4A[*a*, *b*]). This further confirms that the overexcitation that is depicted in the imbalance is real in the neural activities of the brain. Volatilized anesthesia reduces the frequency of spikes and this was confirmed throughout the entire period of recording in TRIM32 WT and KO mice. This observation is documented in a previous study (Antkowiak 1999).

Neurons are the structural and functional units of the nervous system, and Nissl bodies are one of the characteristic structures of neurons. As a measure of neuron integrity after observing overexcitation, whole coronal sections of brain slides stained with Nissl stain estimated the numerical differences of Nissl bodies in the cortex, CA1, CA3, and DG regions of the brain in TRIM32 KO and their WT littermates. There was a significant decrease in neuron numbers in TRIM32 KO mice in all the four brain regions stained (Fig. 4B[*a*–*e*], $P < 0.05, 0.01$), and this could result from excitotoxicity.

The importance of local field potentials (LFPs) has recently surfaced due to the belief that they are linked with certain neural happenings or underpinnings such as visual neurons in the frontal eye field picking signals from distractors as if they were the actual targets (Heitz et al. 2010). Neurons are believed to give off some transmembrane currents which are believed to be LFPs (Destexhe and Bédard 2015). Hence, separating and analyzing frequency oscillations (from 0.1 to 300 Hz) could provide information on whether TRIM32 affects LFPs. The overall LFP is a representative recording from synapses that are formed. The filtering showed a significant reduction of LFPs in the TRIM32 KO mice (Fig. 4C[*a*–c], $P < 0.01$), an observation that corroborates the reduction in the number of neurons as stained by Nissl bodies above.

The Network Activity at Specific Oscillatory Frequency Bands Are Impaired in TRIM32 KO

Neural data recorded and analyzed from specific bandwidth were analyzed to know the effect of TRIM32 KO on the various wave classifications. Bandpass analyzed was classified within the following range of oscillations: Delta waves (0–4 Hz), Theta waves (4–7 Hz), Alpha waves (7–13 Hz), Beta waves (14–30 Hz), and Gamma waves (30–80 Hz). Power spectra of Delta and Beta waves were significantly increased in TRIM32 KO mice, whereas power spectra of Theta and Gamma waves were significantly reduced in TRIM32 KO mice (Fig. 5[*a*–c], $P < 0.01, 0.001$). The decrease in Theta and Gamma waves in this study implies learning and memory deficits (impaired synaptic plasticity). An observation, consistent with the LTP results in our study (Fig. 1A[*a*–c]), suggesting reduced synaptic function in TRIM32 KO mice.

TRIM32 Deficiency Leads to Notch Activation, and Inhibition with DAPT Reverses This Observation

Notch is a regulator of cell cycle exit and it is also a cell's fate determinant just like TRIM32. Studies have suggested that when notch is genetically manipulated, plasticity (functional and structural), as well as behavior, is influenced (Ables et al. 2011). Other roles of notch such as its involvement in the development of the cerebral cortex have been reported (Breunig et al. 2007). Notch is also involved in neurite development (Šestan et al. 1999). Herein, we investigated the possible link between TRIM32 expression and some notch signaling pathway elements concerning the synaptic alterations observed. Notch-related genes such as Notch1, Hes1, and Ngn3 at the mRNA and protein expression levels were examined. Protein and mRNA expressions of these genes were upregulated in TRIM32 KO mice (Fig. 6A[*a*–c], $P < 0.05, 0.01, 0.0001$). In contrast, the general inverse relationship reported between Hes1 and Ngn3 in the canonical Notch pathway in a review by Ables and colleagues was not observed in our study. A probe for a possible reason for this observation revealed that there exists a relationship between Ngn3 and the neurotrophic factor NGF in the brain (Salama-Cohen et al. 2006). mRNA and protein expressions of NGF were significantly downregulated in TRIM32 KO mice in our study (Fig. 6A[*a*–c]). To investigate the expression of mash1 in TRIM32, our results indicate that mRNA expression of mash1 was significantly downregulated in TRIM32 KO (Fig. 6A[*d*, *e*]).

The upregulation of notch signaling genes in TRIM32 KO mice suggested a mechanistic relationship between TRIM32 and notch. This mechanism could result in the observed phenotype in our study. DAPT (a gamma-secretase inhibitor) is well-known to inhibit notch. Treating primary cultured neurons with DAPT revealed a concentration-dependent downregulation of notch1, hes1, ngn3 mRNA, and protein expressions (Fig. 6B and C). Neurotrophic factor, NGF, however, remained unchanged after treatment with DAPT (in all concentrations) (Fig. 6B). A proneural basic helix-loop-helix transcription factor, mash1, was also found to be upregulated in a concentration-dependent manner (Fig. 6B).

Inhibition with DAPT Reduces the Glutamatergic Phenotypes in Primary Neuron Culture

Glutamatergic factors or receptors, one of the hallmarks of overexcitation, were determined. AMPA and NMDA (NR1, NR2A, and NR2B) receptors were significantly downregulated in DAPT-treated neurons. $GABA_A$ receptors were also downregulated but could not be compared with the decrease in the AMPA and NMDA receptors (Fig. 7A[*a*, *b*]). In contrast, mRNA expressions remained unchanged (no significant difference) in all the groups after treatment with DAPT (Fig. 7A[c, *d*]. The overall effect of these on the excitatory and inhibitory transporters was also determined. EAAT2 and SLC32A1 were downregulated and upregulated, respectively, after treatment with DAPT (Fig. 7B[*a*, *b*]. Immunostaining with antibodies reactive against these transporters produced similar outcomes after treatment (Fig. 7B[c–e]).

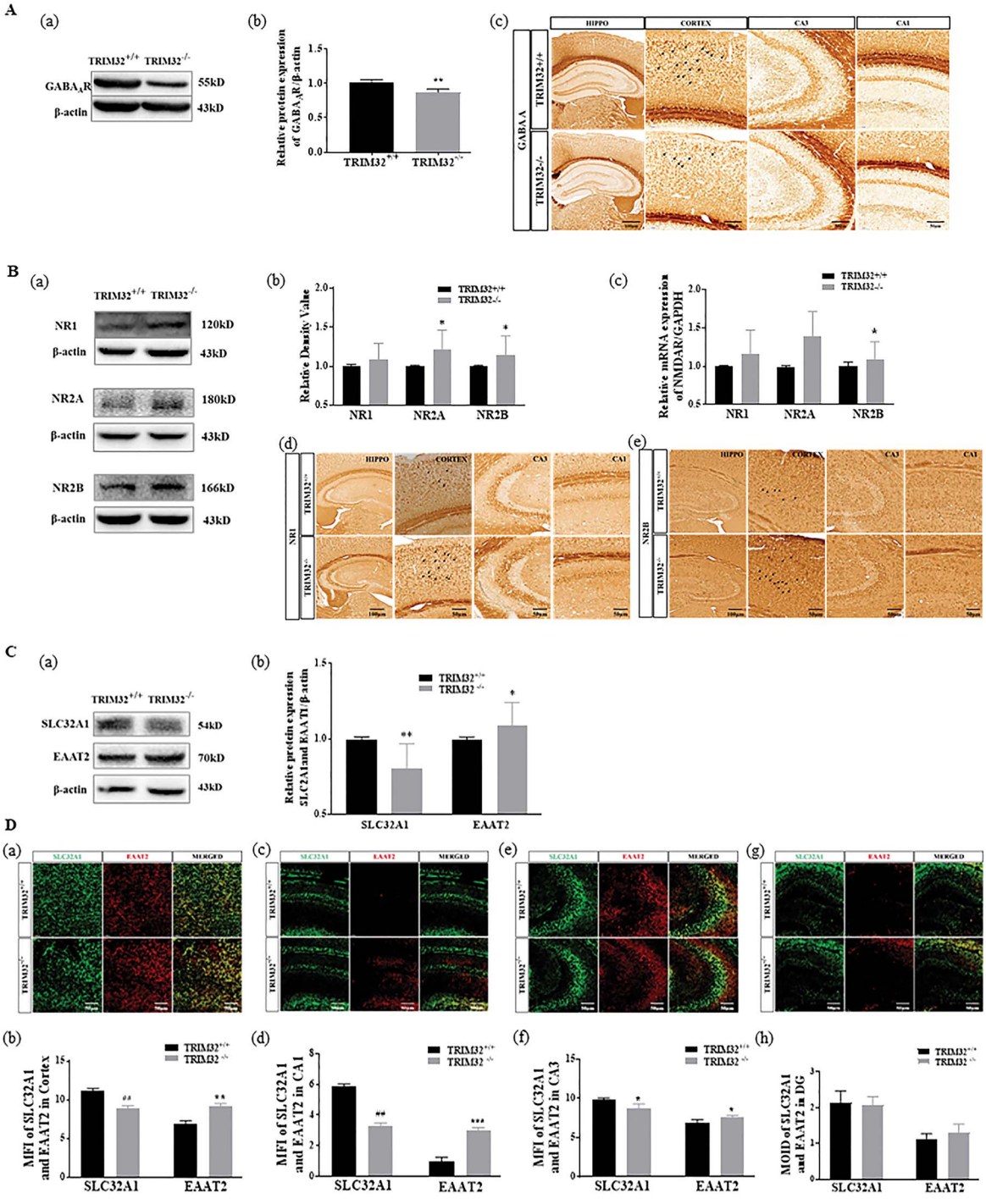

Figure 3. TRIM32KO modulate GABA and NMDA receptors resulting in loss of balance in neurotransporters. (*A*) $GABA_A$ receptor expression is reduced in TRIM32 KO. (*a*) Representative immunoblots and (*b*) densitometry analyses showing downregulation of $GABA_A$ receptor expression. (*c*) Coronal sections of the brain were immunohistochemically stained with antibodies against $GABA_A$. (*B*) NMDA receptor subunits NR1, NR2A, and NR2B are increased in TRIM32 KO. (*a*) Representative immunoblots and (*b*) densitometry analyses of the immunoblots showed that the protein expression levels of NR1, NR2A, and NR2B increased in TRIM32 32 KO mice with NR2A and NR2B being significant. (*c*) Relative mRNA expression of RT-qPCR showed that expression levels of nr1, nr2a, nr2b increased in TRIM32 KO mice with nr2a being significant (at least 10 brain samples in each group). (*d*, *e*) Coronal sections of the brain were immunohistochemically stained with antibodies specific to NR1 and NR2B (3 mice in each group). (*C*) Whole hippocampal brain lysates showing the expression of excitatory and inhibitory transporters (*a*) Representative immunoblots and (*b*) densitometry analyses showing the protein expressions of EAAT2 and SLC32A1. (*D*) Brain-specific portions showing the expression of excitatory and inhibitory transporters. (*a*–*h*) Coronal sections of the Cortex, CA1, CA3, and DG were immunofluorescent stained with antibodies against SLC32A1 and EAAT2 (Green: SLC32A1; Red: EAAT2) and the mean fluorescent intensity (MFI) of their immunoreactivity was quantified. Here, NR1, NR2A, NR2B, SLC32A1, EAAT2, and their corresponding β-actin immunoblots were performed on different parts of the PVDF membrane of different gels; NR1, NR2A, NR2B, SLC32A1, and EAAT2 were normalized to the respective β-actin, whereas NR1, NR2A, and NR2B were normalized to GAPDH in the mRNA expression. Data (means ± SEM) are from at least three independent cohorts of WT littermates ($n = 3$). $^*P < 0.05$, $^{**}P < 0.01$, $^{***}P < 0.001$, $^{\#\#}P < 0.0001$.Data are means ± SEM from at least three independent cohorts of mice littermates ($n = 3$).

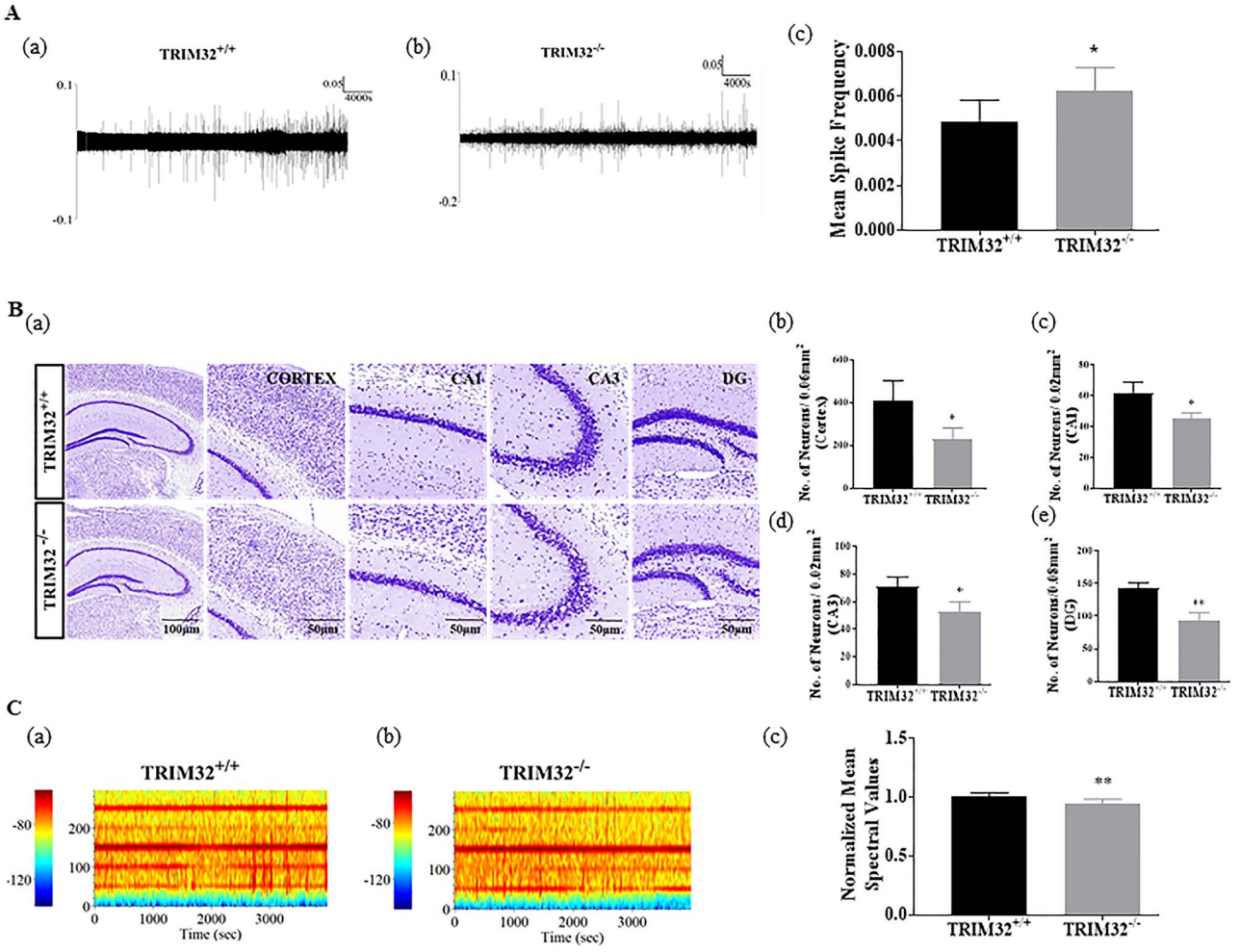

Figure 4. Over excitation leads to an increase in the frequency of spikes and loss of neurons in TRIM32 KO mice. (*A*) The frequency of spikes is increased in TRIM32 KO mice. (*a*, *b*) Representative traces of spikes generated in TRIM32 KO mice and their WT littermates within 4000 s of recording. There were no spike clusters or bursts, confirming the effect of volatile anesthetics on spike generation. (*c*) Mean spike frequency analyzed with Instant frequency showed a significant increase in TRIM32 KO mice compared with the WT. (*B*) Overexcitation leads to loss of neurons. (*a*) Representative images of Nissl staining showing the differences in the neuron numbers in the Cortex, CA1, CA3, and DG of TRIM32 KO and WT mice brain. (*b–e*) Bar graph representation of estimated neuron numbers in the Cortex, CA1, CA3, and DG regions, respectively. (*C*) LFPs are generated from Neuron's transmembrane within a frequency range of 0.1–300 Hz. Representative spectrograms showed that spectral colors are (*a*) higher in TRIM32 WT and (*b*) lower in TRIM32 KO mice. (*c*) Normalized differential band spectrum decreased significantly in TRIM32 KO mice. Data are presented as means ± SEM from at least three independent animals ($n = 3$) and at least nine mice per group for neural data acquisition. $^{*}P < 0.05$, $^{**}P < 0.01$.

Discussion

TRIM32 is a kind of NSC-related protein that plays an important role in the development of rat neocortex. It has also been found to regulate NSC proliferation and neuronal differentiation (Hillje et al. 2013). The expression of TRIM32 protein can induce NSCs to produce neurons. The uncertainty about the effect of TRIM32 on synaptic plasticity and the mechanism involved needs to be unraveled. This study, therefore, demonstrates for the first time that TRIM32 directly or indirectly alters synaptic plasticity and has proposed possible mechanisms involved. In the process of evolution, animals, especially humans, have survived and adapted to environmental changes using their learning ability. The body can produce certain adaptive responses that make the brain form neural circuits during the adaptation process and this is known as plasticity (Sherwood et al. 2008). Synaptic plasticity plays an important role in many physiological and pathological processes such as the development of the nervous system, learning and memory, and nerve damage and repair. The changes that occur in the synaptic connections tend to become the structural basis for learning and memory functions. LTP has been widely accepted as an experimental model of synaptic plasticity and has been widely used by neuroscientists.

In this current study, the long-term synaptic plasticity (as recorded by LTP experiment) was impaired in TRIM32 KO mice, whereas the short-term synaptic plasticity did not change according to the PPF curve. This is an indication that the release of the SVs remained unchanged. The I/O curve depicts synaptic transmission efficiency, and our results also confirm that the basal synaptic transmission of neurons is efficient. This implies that knockout of TRIM32 does not affect the synaptic transmission efficiency. Dendritic spines tend to receive synaptic contacts that usually change when new experiences are encountered. This is a necessity for the processes of structural plasticity. It had been previously held

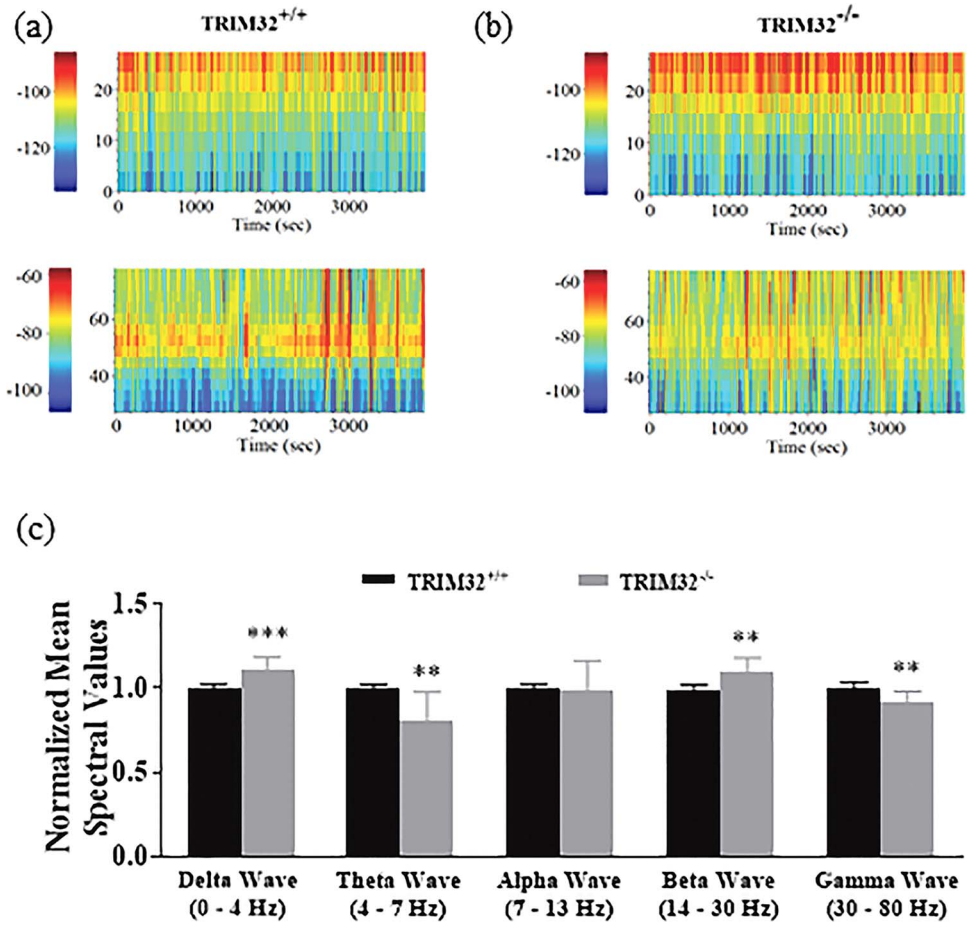

Figure 5. Altered network activity at specific oscillatory frequency bands in TRIM32 KO. EEG recordings with the various oscillatory bands are affected in TRIM32 KO mice and showed patterns that are associated with certain neurological disorders. (*a*, *b*) Representative spectrograms showing spectral colors of Delta and Beta oscillations are relatively higher whereas those of Theta and Gamma oscillations are lower in TRIM32 KO mice. (*c*) Normalized differential band spectrum showed significant effects in Delta, Theta, Beta, and Gamma waves in WT and TRIM32 KO mice under volatile anesthesia. Delta and Beta oscillations or rhythms are increased significantly, whereas Theta and Gamma oscillations or rhythms are decreased significantly in TRIM32 KO mice. Data represent mean ± SEM from at least nine mice per group. $^{*}P < 0.05$; $^{**}P < 0.01$; $^{***}P < 0.001$.

that spine density matches with synaptic plasticity. However, recent findings have proposed that morphological changes that occur within the spine are of much importance for new learning and memory formation than total spine number or density (van der Zee 2015). Dendritic spine density in TRIM32 KO mice decreased particularly in the CA1 and CA3 areas of the hippocampus (Fig. 1B[*a*–*c*]), and this may contribute to the impaired LTP we observed. The mushroom type of spines is typical of neuronal networks undergoing significant restructuring and maturation (Risher et al. 2014). In this study, a significant reduction in the number of mushroom spines is observed in the CA1 and CA3 areas of the hippocampus in the absence of TRIM32. A study reported that AMPA type of glutamate receptors is abundant in the mushroom spines and could be sparsely distributed in the spines or Filopodia (Bourne and Harris 2008). This observation is consistent with our reduced AMPAR expression in TRIM32 KO mice reported in this study. It has been reported several times that smaller thin spines may generally be considered weaker in function especially due to their lower density of glutamate receptors (Yan et al. 2019). It is noteworthy that the dendrite morphology of the TRIM32 KO mice had a slender and long neck and the bulbs were much smaller. Conversely, the WT dendrite spines were more clustered and had some branches, consistent with reports that clusters of dendritic spines are essential for strengthening synapses (Gipson and Olive 2017).

Many proteins are found in the presynaptic or postsynaptic site of neurons and mostly involved in either the generation or release of neurotransmitters by interacting with each other and may form complex networks that take part in synapse formation, their maintenance, and function. In this study, synaptic proteins (synaptophysin, Synapsin1, GAP-43, and PSD95) were all downregulated in the TRIM32 KO mice hippocampus. Numerous reports have suggested that tyrosine phosphorylation of synaptophysin (syp) is a requirement for LTP formation (Evans and Cousin 2005), whereas other reports have suggested that syp is not the only requirements for SV cycle; hence, its function in determining synaptic strength cannot be overlooked (Schmitt et al. 2009). Synapsin has been extensively studied concerning their function in the SV life cycle (Mirza and Zahid 2018). Recently, researchers have suggested that they affect SV pools and lead to inhibition and slowing of neurotransmitter release

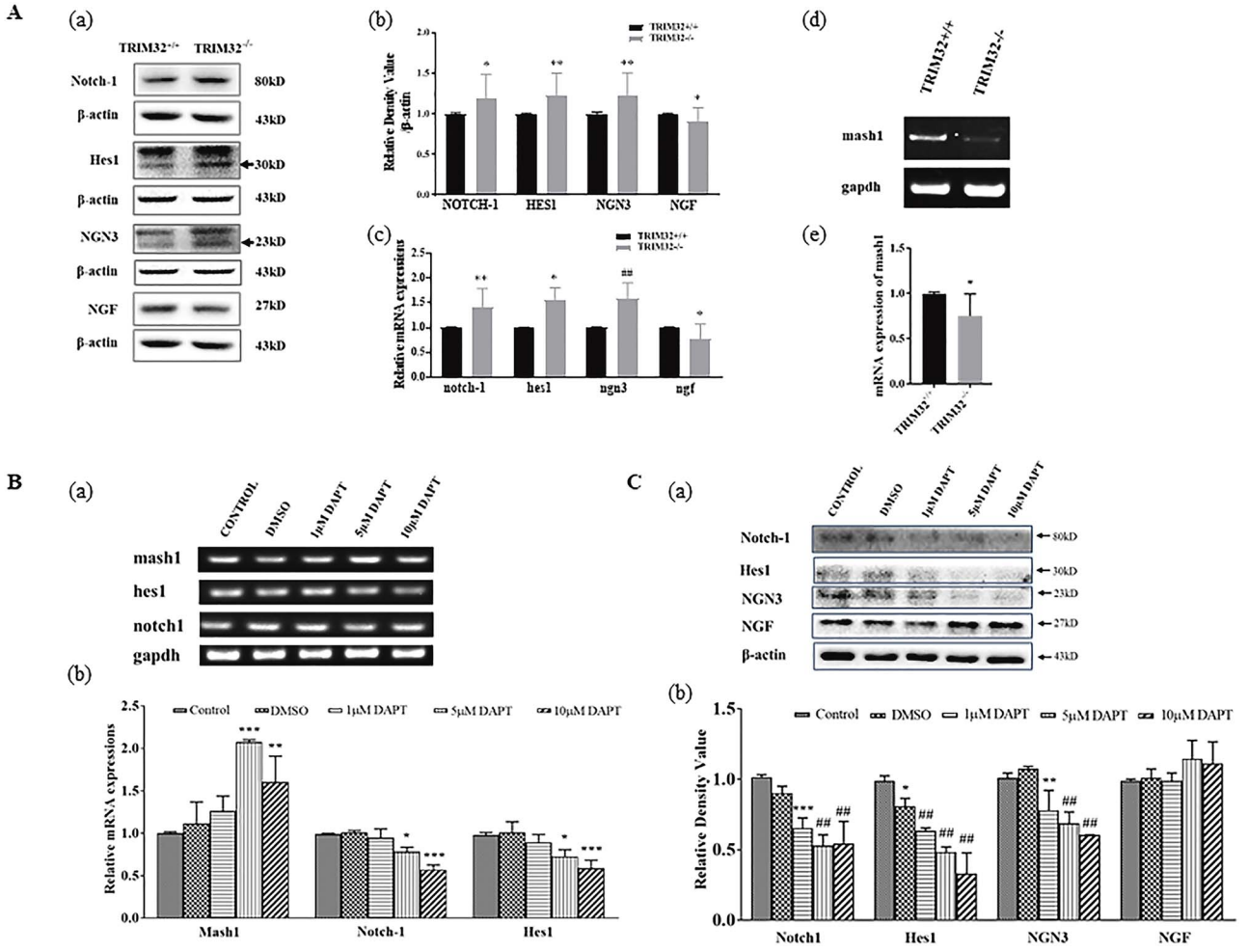

Figure 6. Changes in the Notch pathway in TRIM32 KO mice. (*A*) TRIM32 deficiency increases the expression of notch1 and some selected pathway genes in the hippocampus. (*a*) Representative immunoblots and (*b*) densitometry analysis of the immunoblots showed significant upregulation of NOTCH1, HES1, and NGN3 in TRIM32 KO mice, whereas NGF was downregulated significantly. (*c*) Relative mRNA expression of RT-qPCR showed expression levels of notch1, hes1, and ngn3 are upregulated in TRIM32 KO mice, whereas NGF is downregulated. (*B*) Notch inhibition with DAPT altered mRNA expressions of downstream genes. (*a*) Representative micrographs of RT-PCR and (*b–d*) densitometry analysis of notch1, hes1, and mash1. (*C*) Notch inhibition with DAPT altered protein expressions of downstream genes. (*a*) Representative immunoblots and (*b–d*) densitometry analysis of the immunoblots showed a significant downregulation of NOTCH1, HES1 and NGN3 in a concentration-dependent manner in vitro, whereas NGF was unchanged. Here, NOTCH1 and NGF whereas HES1 and NGN3 (*A*); NOTCH1 and HES1 whereas NGF and NGN3 (*C*) were performed on different parts of the PVDF membrane of the same gels and were normalized to their respective β-actin. In the RT-PCR notch1, hes1, ngn3, ngf, and mash1 were normalized to GAPDH. Data represent mean ± SEM from 10 mice per group. $^{*}P < 0.05$; $^{**}P < 0.01$; $^{***}P < 0.001$; $^{\#\#}P < 0.0001$.

kinetics (Baldelli et al. 2007). They have also been reported to result in an imbalance between excitatory and inhibitory activities of neurons (Chiappalone et al. 2008). This observation is also reported in our study. Many studies have also reported the effect of GAP-43 on the release of neurotransmitters and synaptic plasticity (Holahan and Routtenberg 2008; Holahan 2015). In a study where PSD-95 was overexpressed in hippocampal neurons, synaptic maturation was enhanced and the converse also resulted in a reduction in synaptic strength and spine density (Hu et al. 2011). Our results of downregulated synaptic proteins in the wake of reduced LTP are consistent with all these studies, as the state of these synaptic proteins in TRIM32 KO mice directly or indirectly leads to impaired LTP. A significant decrease in the expression of the AMPAR (Fig. 2C[*a–c*]) observed supports the impaired LTP reported in this study. The mechanism of LTP activation involves the release of glutamic acid from the presynaptic neuron which first binds to an AMPAR on the postsynaptic neuron membrane and the NMDA receptor. The AMPAR activates the depolarization of the cell membrane and causes the removal of Mg^{2+} obstructing the NMDA receptor channel. The release of Mg^{2+} causes Ca^{2+} to enter the postsynaptic neurons, and the influx of Ca^{2+} determines the strength of LTP. Therefore, when AMPARs are less, the formation of LTP is presumed weakened. It has been reported that the recruitment of calcium-permeable (GluA2-lacking) AMPARs is profound in mushroom-type spines in hippocampal CA1 neurons (Matsuo et al. 2008). This explains the decrease in AMPARs in the TRIM32 KO mice and the corresponding impaired LTP observed in this study.

GABA receptors can inhibit neuronal hyperexcitability. Neuronal inhibitory $GABA_A$ receptors mediate two different electrophysiological effects: the phasic and tonic inhibitions (Chang et al. 2018). In the course of pathological development, GABA receptors do not act alone but interact with other receptors.

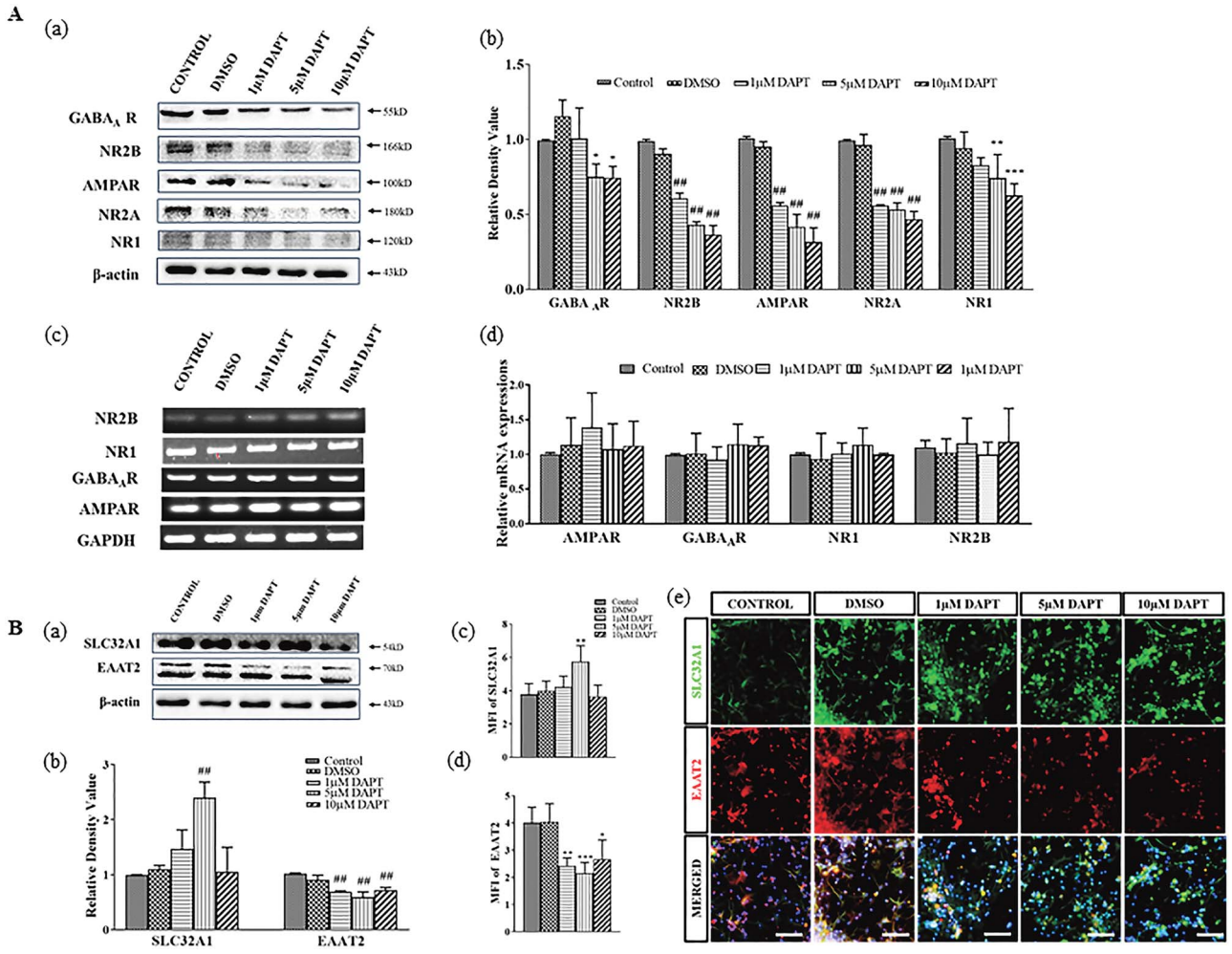

Figure 7. Notch inhibition with different concentrations of DAPT, influenced GABA and NMDA receptors expressions, and restored balance in neuronal transmission and excitability. (*A*) GABAergic phenotype is marginally reduced and glutamatergic is drastically downregulated in a concentration-dependent manner in cell lysates. Representative immunoblots (*a*) and densitometry (*b*) analyses showing the protein expression of $GABA_A$, NR2B, AMPA, NR2A, and NR1 receptors. Representative bands (*c*) and densitometry analyses (*d*) showing the mRNA expression of NR1, NR2B, GABA, and AMPARs. (*B*) Changes in the expression of excitatory (EAAT2) and inhibitory (SLC32A1) transporters after DAPT treatment. (*a*) Representative immunoblots and (*b*) densitometry analyses showing the protein expressions of EAAT2 and SLC32A1 in cell lysates. (*c*, *d*) MFI of cells stained with antibodies against SLC32A1 and EAAT2. (*e*) Cells were immunofluorescent stained with antibodies against SLC32A1 (Green) and EAAT2 (Red). Scale bar: 5 μm. Data are means ± SEM from at least three independent cell experiments of different concentrations. $^*P < 0.05$, $^{**}P < 0.01$, $^{***}P < 0.001$, $^{\#\#}P < 0.0001$.

Therefore, the decreased expression of the $GABA_A$ receptor in TRIM32 KO mice could also be a major factor contributing to LTP decline. Glutamic acid released from the presynaptic membrane triggers a role in the receptor on the postsynaptic membrane which participates in synaptic plasticity, long-term potentiation as well as signal transduction. The increase in NR1, NR2A, and NR2B (NMDA Receptor subunits) in TRIM32 KO mice and the impaired LTP seem to support the detrimental effect of over-expressed NMDARs on synaptic plasticity in this study. Even though many studies have reported that synaptic NMDARs are important for LTP; extrasynaptic NMDARs can trigger de novo long-term depression (LTD) under certain conditions (Massey et al. 2004). Okamoto and his group reported that increased extrasynaptic NMDA activity has a deleterious effect in mouse models of Huntington's disease and other neurological disorders (Okamoto et al. 2009; Milnerwood et al. 2010). The observed increase in NMDARs is indicative of increased excitation which possibly affected neuronal stability, resulting in reduced neuronal number, and subsequently causing a deficit in synaptic plasticity in TRIM32 KO mice (Xu et al. 2019). Li et al. reported that soluble Aβ oligomers at the pathophysiological levels present in the AD brain facilitate hippocampal LTD (impaired learning and memory) by increasing the activation of NR2B-containing extrasynaptic NMDARs (Li et al. 2009).

One of the most widely accepted hypotheses regarding autism is the proposal that there is an excitatory-inhibitory (E-I) imbalance in the brain neural circuits. This imbalance has been the cause of social, behavioral, emotional, cognitive, sensory, and motor control deficits. Some studies have used optogenetics and have reported that increased E-I ratio in the prefrontal cortex results in social and behavioral impairment that is observed in ASD (Yizhar et al. 2011). TRIM32 gene mutation has been highly linked to Autism (Zhu et al. 2019). There is difficulty in studying E-I imbalance in humans; hence, most of the knowledge about

this are mainly from animal models which are believed to mainly overlap with humans. E-I imbalance has been reported to occur when there is an increase in glutamatergic or a decrease in GABAergic signaling (Opris and Casanova 2014). Glutamatergic transmission higher than GABAergic transmission is revealed by the expressions of EAAT2 and SLC32A1 proteins (Fig. 3C and D) in our study. This imbalance has been reported to alter synaptic plasticity (Bateup et al. 2013). This corroborates the impaired LTP in TRIM32 KO mice. The decrease in GABA receptor earlier reported confirms this observation and can lead to neuronal hyperexcitability.

The imbalance or overexcitation could also be confirmed by the results obtained from this study, in which the spiking frequency was observed to be higher in the TRIM32 KO mice. Even though the number of spikes was typically low, the difference was significantly clear and confirms the observation that results from animals under volatile anesthetics generally have reduced neural and synaptic activities in the CNS (Antkowiak 1999). With the reduced neuronal numbers in the various parts of the brain of TRIM32 KO mice (Fig. 4B[a–e]) and the neuronal hyperexcitability explained above, a decrease in neuronal number is not farfetched. The importance of LFPs has recently surfaced due to the belief that they are linked with certain neural happenings or underpinnings (Heitz et al. 2010). Neurons give off some transmembrane currents which are known to be LFPs (Destexhe and Bédard 2015). This reduced neuronal numbers could indicate TRIM32 effects on LFPs. LFP has been proposed to be a reflection of local synaptic activities (Kaur et al. 2004). Hence, the results from this study showing reduced LFP in the TRIM32 KO mice (Fig. 2F–*H*) are consistent with the reduced synaptic activities that are expected to affect synaptic plasticity.

The overall outcome of modifications in synaptic plasticity needed to be looked at in the light of possible effects on the brain function. In this study, Delta waves were found to increase in TRIM32 KO mice. This result is consistent with numerous studies that have associated disruptions in delta waves found in diseases such as Ischemic brain diseases (Inui et al. 1994), dementia (Yudofsky et al. 2002), sleep disorders (Pilon et al. 2006), schizophrenia (Alfimova and Uvarova 2007), and Parkinson's disease (Yudofsky et al. 2002). The results obtained also showed reduced Theta and gamma waves in the TRIM32 KO mice, indicating impaired synaptic plasticity. There have been reports that increased theta-related firing, which helps to strengthen the connections between spatially distributed neurons and thereby improving memory (Paz et al. 2008), a result that can explain the observation that was made during this study. Gamma oscillations have for a long time been thought to be very crucial for advance cognitive functions as well as sensory responses (Buzsaki et al. 2003; Fries et al. 2007). These observations may be associated with the altered synaptic plasticity in TRIM32 KO mice.

In normal brain development, differentiation mechanisms require a very accurate timing, and Notch signaling has been studied as one of the master regulators of NSCs and neurogenesis (Qi et al. 1999; Louvi and Artavanis-Tsakonas 2006). Mutations in some Notch elements have been linked to diseases such as Down's syndrome and Alzheimer's disease, and these confer synaptic plasticity impairment. This impairment in synaptic plasticity has been supported by our results. While high levels of notch keep cells in a quiescent state, a decrease in Notch activity leads to an increase in the net number of adult neurons (Chapouton et al. 2010). Our results showed an upregulation in Notch-1 in TRIM32 KO mice (Fig. 6) and a decrease in the number of neurons (Fig. 4). It has been reported that an increase in Notch induces the overexpression of Hes1 or Hes5 and this, in turn, inhibits neurogenesis and promotes astrogliogenesis (Wu et al. 2003; Kageyama et al. 2008, 2009). This finding agrees with the results we obtained where upregulation in Notch-1 in TRIM32 KO also led to an increase in Hes1 in both the mRNA and the protein expression levels as well as mRNA expression levels mash1 in TRIM32 KO were downregulated. A similar observation has also been reported by Salama-Cohen et al. 2005, where they concluded that the activation of Notch increased the expression of Hes1/5 genes. Another research by the same group reported that strong activation of Notch by high cell density reduced the expression of Ngn3, which agrees with the report that Ngn3 and Mash1 are negatively controlled by Notch, and its nuclear targets, Hes1 and Hes5 (Kageyama and Nakanishi 1997). Our results, however, reveal a contrary opinion where the upregulation of Notch-1 and Hes1 in TRIM32 KO led to an increase in Ngn3 both at the mRNA and protein expression levels. This necessitated the search for a reason for this observation. A study by Salama-Cohen et al. 2006 reported that NGF downregulates Ngn3. This indicated that NGF can control the expression of Ngn3 through other pathways. This is what led us to determine the expression levels of NGF at the mRNA levels and the results showed a decrease in ngf mRNA in TRIM32 KO mice. This was further confirmed at the protein expression levels where NGF was significantly downregulated in TRIM32 KO mice. Our findings suggest that NGF is antagonistic to Ngn3 in the absence of TRIM32. A study reported that the overexpression of Ngn3 led to a decrease in the number of synaptic contacts thereby suppressing the number of inhibitory terminals. A finding is also confirmed by this study where inhibitory contacts marker SLC32A1 (Fig. 3C and *D*) was markedly reduced in TRIM32 KO (which had increased Ngn3) (Salama-Cohen et al. 2006). Overexpression of Ngn3 leads to the downregulation of Mash1 and in turn leads to the reduced number of GABAergic synaptic terminals (Roybon et al. 2010) to about half of the control levels, whereas the glutamatergic synaptic terminals increased. This observation is confirmed by our experiment where the inhibition of notch downregulated downstream genes leading to the upregulation of mash1. A couple of studies has shown that the loss of GABAergic phenotype specification is mash1-dependent (Parras et al. 2002; Roybon et al. 2010). In as much, neurogenins and mash1 are believed to be expressed in ways complementary to each other in the dorsal and ventral telencephalon and this contributes to the generation of glutamatergic and GABAergic neurons (Parras et al. 2002). Therefore, the conclusion that higher levels of Ngn3 (leading to lower levels of mash1) will increase the network activity in developing neuronal circuits and the distortions in the E/I balance could be supported by our results (which showed higher excitatory transmission and lower inhibitory transmission) (Fig. 3C and *D*). All these observations have been linked to decreased synaptic plasticity (Fig. 8).

In summary, this study demonstrates the effects of TRIM32 on synaptic function and reports on changes in hippocampal synaptic plasticity. LTP impairment, reduced dendritic spines, downregulation of synaptic plasticity-related proteins, imbalance in excitation and inhibition phenotypes leading to reduced neuronal number, as well as changes in EEG waves have been explored. Finally, there is evidence that the expression of notch and its related elements may be responsible for impaired synaptic plasticity in TRIM32 KO mice and that notch inhibition with DAPT could improve synaptic plasticity outcomes. A study showed that notch inhibition with DAPT improved learning and

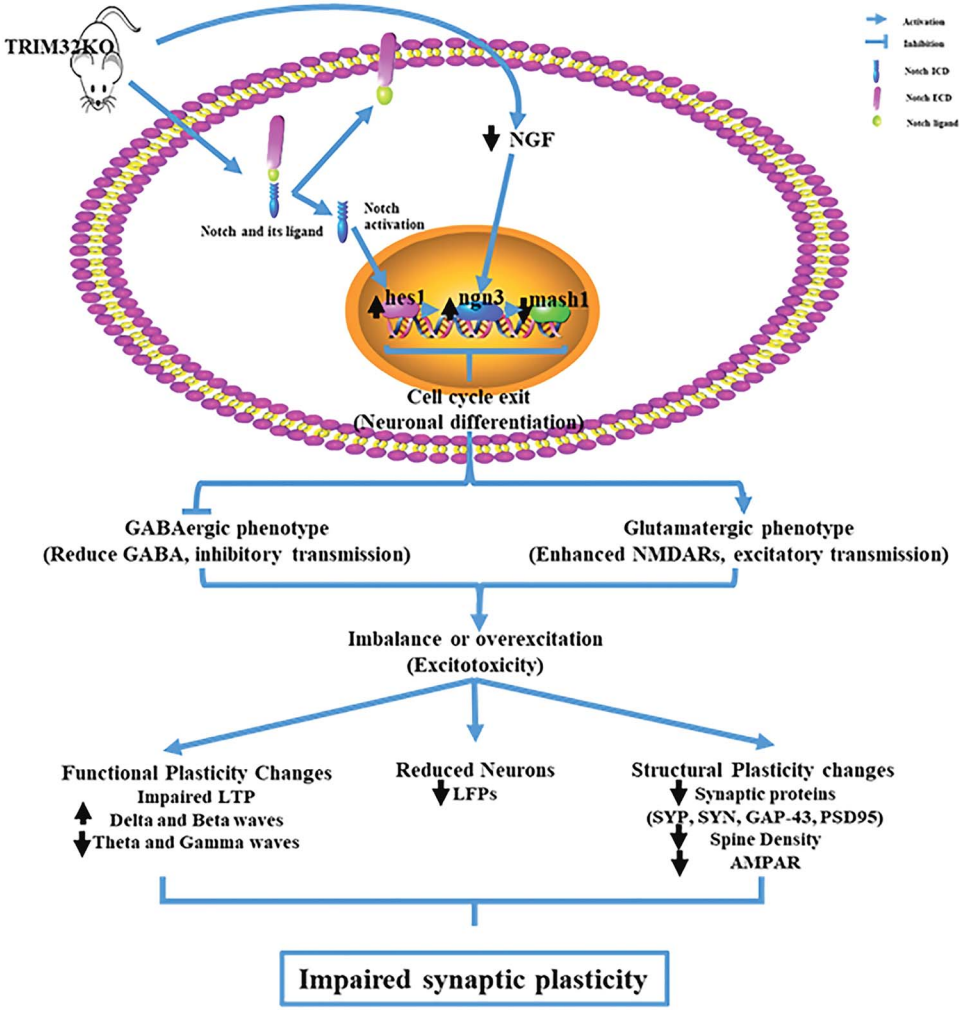

Figure 8. Proposed pathway representing the mechanistic relationship between TRIM32 and notch signaling and its resultant effects on synaptic plasticity.

memory abilities in craniocerebral injured rats (Zhang et al. 2018). Further studies are required to ascertain a conclusive relationship between TRIM32 and the notch pathway by inhibiting notch in vivo to see the effects on functional learning and memory outcomes.

Authors Contributions

S.L., J.Z., and Q.-H.M. contributed to the conception and design of the project. M.N., Q.-F.L., Y.Z., X.-D.L., N.L., X.Z., H.-L.S., B.K., B.W., Q.W., K.K., and X.-F.W. contributed to the conduct of the experiments and analysis of data. M.N. wrote the manuscript. W.W. helped with manuscript revision and proofread. All authors read and approved the final version of manuscript.

Funding

Liaoning Provincial Key R&D Program (2019020048-JH2/103); Liaoning Revitalization Talents Program (XLYC1902044, XLYC1808031); National Major Scientific and Technological Special Project for "Significant New Drugs Development" (2019zx09301102); National Natural Sciences Foundation of China (81571061, 81671061, 81671111, and 81870897); Natural Science Foundation of Jiangsu Province (BK20181436). However, they did not influence the study design, data interpretation, and/or manuscript preparation.

Notes

Conflict of interest: The authors declare that they have no competing interest in this publication.

References

Ables JL, Breunig JJ, Eisch AJ, Rakic P. 2011. Not (ch) just development: Notch signaling in the adult brain. *Nature Reviews Neuroscience*. 12(5):269.

Alfimova MV, Uvarova LG. 2007. Changes in the EEG spectral power during perception of neutral and emotionally salient words in schizophrenic patients, their relatives and healthy individuals from the general population. *Zhurnal vysshei nervnoi deiatelnosti imeni IP Pavlova*. 57(4):426–436.

Antkowiak B. 1999. Different actions of general anesthetics on the firing patterns of neocortical neurons mediated by the GABAAReceptor. *Anesthesiology: The Journal of the American Society of Anesthesiologists*. 91(2):500–511.

Baldelli P, Fassio A, Valtorta F, Benfenati F. 2007. Lack of synapsin I reduces the readily releasable pool of synaptic vesicles at central inhibitory synapses. *Journal of Neuroscience*. 27(49):13520–13531.

Bateup HS, Johnson CA, Denefrio CL, Saulnier JL, Kornacker K, Sabatini BL. 2013. Excitatory/inhibitory synaptic imbalance leads to hippocampal hyperexcitability in mouse models of tuberous sclerosis. *Neuron*. 78(3):510–522.

Breunig JJ, Silbereis J, Vaccarino FM, Šestan N, Rakic P. 2007. Notch regulates cell fate and dendrite morphology of newborn neurons in the postnatal dentate gyrus. *Proceedings of the National Academy of Sciences*. 104(51):20558–20563.

Bourne JN, Harris KM. 2008. Balancing structure and function at hippocampal dendritic spines. *Annual Review of Neuroscience*. 31:47–67.

Buzsáki G, Buhl DL, Harris KD, Csicsvari J, Czeh B, Morozov A. 2003. Hippocampal network patterns of activity in the mouse. *Neuroscience*. 116(1):201–211.

Chang YY, Gong XW, Gong HQ, Liang PJ, Zhang PM, Lu QC. 2018. GABAA receptor activity suppresses the transition from inter-ictal to Ictal Epileptiform discharges in juvenile mouse hippocampus. *Neurosci Bulletin*. 34:1007–1016.

Chapouton P, Skupien P, Hesl B, Coolen M, Moore JC, Madelaine R, Kremmer E, Faus-Kessler T, Blader P, Lawson ND, et al. 2010. Notch activity levels control the balance between quiescence and recruitment of adult neural stem cells. *Journal of Neuroscience*. 30(23):7961–7974.

Chiappalone M, Casagrande S, Tedesco M, Valtorta F, Baldelli P, Martinoia S, et al. 2008. Opposite changes in glutamatergic and GABAergic transmission underlie the diffuse hyperexcitability of synapsin I–deficient cortical networks. *Cerebral Cortex*. 19(6):1422–1439.

Destexhe A, Bédard C. 2015. Local field potentials (LFP). *Encyclopedia of Computational Neuroscience*. 1591–1601. doi: 10.1007/978-1-4614-6675-8_548.

Evans G, Cousin M. 2005. Tyrosine phosphorylation of synaptophysin in synaptic vesicle recycling. Portland Press Limited. *Biochemical Society Transactions*. 33:1350–1353.

Fries P, Nikoli, ć D, Singer W. 2007. The gamma cycle. *Trends in Neurosciences*. 30:309–316.

Gipson CD, Olive MF. 2017. Structural and functional plasticity of dendritic spines–root or result of behavior? *Genes, Brain, and Behavior*. 16(1):101–117.

Heitz RP, Cohen JY, Woodman GF, Schall JD. 2010. Neural correlates of correct and errant attentional selection revealed through N2pc and frontal eye field activity. *Journal of Neurophysiology*. 104(5):2433–2441.

Hillje AL, Beckmann E, Pavlou MA, Jaeger C, Pacheco MP, Sauter T, Schwamborn JC, Lewejohann L. 2015. The neural stem cell fate determinant TRIM32 regulates complex behavioral traits. *Frontiers in Cellular Neuroscience*. 9:75.

Hillje AL, Pavlou MA, Beckmann E, Worlitzer MM, Bahnassawy L, Lewejohann L, Palm T, Schwamborn JC. 2013. TRIM32-dependent transcription in adult neural progenitor cells regulates neuronal differentiation. *Cell Death & Disease*. 4(12):e976.

Holahan M, Routtenberg A. 2008. The protein kinase C phosphorylation site on GAP-43 differentially regulates information storage. *Hippocampus*. 18(11):1099–1102.

Holahan MR. 2015. GAP-43 in synaptic plasticity: molecular perspectives. *Research and Reports in Biochemistry*. 5: 137–146.

Hu X, Ballo L, Pietila L, Viesselmann C, Ballweg J, Lumbard D, Stevenson M, Merriam E, Dent EW. 2011. BDNF-induced increase of PSD-95 in dendritic spines requires dynamic microtubule invasions. *Journal of Neuroscience*. 31(43):15597–15603.

Inui K, Kawamoto H, Kawakita M, Wako K, Nakashima H, Kamihara M, Nomura J. 1994. Temporal delta wave and ischemic lesions on MRI. *Psychiatry and Clinical Neurosciences*. 48(4):891–898.

Kageyama R, Nakanishi S. 1997. Helix-loop-helix factors in growth and differentiation of the vertebrate nervous system. *Current Opinion in Genetics & Development*. 7(5):659–665.

Kageyama R, Ohtsuka T, Kobayashi T. 2008. Roles of Hes genes in neural development. *Development, Growth & Differentiation*. 50:S97–S103.

Kageyama R, Ohtsuka T, Shimojo H, Imayoshi I. 2009. Dynamic regulation of notch signaling in neural progenitor cells. *Current Opinion in Cell Biology*. 21(6):733–740.

Kasai H, Hayama T, Ishikawa M, Watanabe S, Yagishita S, Noguchi J. 2010. Learning rules and persistence of dendritic spines. *European Journal of Neuroscience*. 32(2): 241–249.

Kaur S, Lazar R, Metherate R. 2004. Intracortical pathways determine breadth of subthreshold frequency receptive fields in primary auditory cortex. *Journal of Neurophysiology*. 91(6):2551–2567.

Li Q, Wu X, Na X, Ge B, Wu Q, Guo X, Ntim M, Zhang Y, Sun Y, Yang J, et al. 2019. Impaired cognitive function and altered hippocampal synaptic plasticity in mice lacking Dermatan Sulfotransferase Chst14/D4st1. *Frontiers in Molecular Neuroscience*. 12:26.

Li S, Hong S, Shepardson NE, Walsh DM, Shankar GM, Selkoe D. 2009. Soluble oligomers of amyloid β protein facilitate hippocampal long-term depression by disrupting neuronal glutamate uptake. *Neuron*. 62(6): 788–801.

Lionel AC, Crosbie J, Barbosa N, Goodale T, Thiruvahindrapuram B, Rickaby J, Gazzellone M, Carson AR, Howe JL, Wang Z, et al. 2011. Rare copy number variation discovery and cross-disorder comparisons identify risk genes for ADHD. *Science Translational Medicine*. 3(95):95ra75.

Lionel AC, Tammimies K, Vaags AK, Rosenfeld JA, Ahn JW, Merico D, Noor A, Runke CK, Pillalamarri VK, Carter MT, et al. 2013. Disruption of the ASTN2/TRIM32 locus at 9q33. 1 is a risk factor in males for autism spectrum disorders, ADHD and other neurodevelopmental phenotypes. *Human Molecular Genetics*. 23(10):2752–2768.

Liu J, Zhang C, Wang XL, Ly P, Belyi V, Xu-Monette ZY, Young KH, Hu W, Feng Z. 2014. E3 ubiquitin ligase TRIM32 negatively regulates tumor suppressor p53 to promote tumorigenesis. *Cell Death and Differentiation*. 21(11):1792.

Louvi A, Artavanis-Tsakonas S. 2006. Notch signalling in vertebrate neural development. *Nature Reviews Neuroscience*. 7(2):93.

Massey PV, Johnson BE, Moult PR, Auberson YP, Brown MW, Molnar E, Collingridge GL, Bashir ZI. 2004. Differential roles of NR2A and NR2B-containing NMDA receptors in cortical long-term potentiation and long-term depression. *Journal of Neuroscience*. 24(36):7821–7828.

Matsuo N, Reijmers L, Mayford M. 2008. Spine-type-specific recruitment of ewly synthesized AMPA receptors with learning. *Science*. 319(5866):1104–1107.

Meroni G, Diez-Roux G. 2005. TRIM/RBCC, a novel class of 'single protein RING finger' E3 ubiquitin ligases. *Bioessays*. 27:1147–1157.

Milnerwood AJ, Gladding CM, Pouladi MA, Kaufman AM, Hines RM, Boyd JD, Ko RW, Vasuta OC, Graham RK, Hayden MR, et al. 2010. Early increase in extrasynaptic NMDA receptor signaling and expression contributes to phenotype onset in Huntington's disease mice. *Neuron*. 65(2):178–190.

Mirza FJ, Zahid S. 2018. The role of synapsins in neurological disorders. *Neurosci Bulletin*. 34:349–358.

Nicklas S, Otto A, Wu X, Miller P, Stelzer S, Wen Y, Kuang S, Wrogemann K, Patel K, Ding H, et al. 2012. TRIM32 regulates skeletal muscle stem cell differentiation and is necessary for normal adult muscle regeneration. *PloS One*. 7(1):30445.

Okamoto SI, Pouladi MA, Talantova M, Yao D, Xia P, Ehrnhoefer DE, Zaidi R, Clemente A, Kaul M, Graham RK, et al. 2009. Balance between synaptic versus extrasynaptic NMDA receptor activity influences inclusions and neurotoxicity of mutant huntingtin. *Nature Medicine*. 15(12):1407.

Opris I, Casanova MF. 2014. Prefrontal cortical minicolumn: from executive control to disrupted cognitive processing. *Brain*. 137(7):1863–1875.

Parras CM, Schuurmans C, Scardigli R, Kim J, Anderson DJ, Guillemot F. 2002. Divergent functions of the proneural genes Mash1 and Ngn2 in the specification of neuronal subtype identity. *Genes Dev*. 16:324–338.

Paz R, Bauer EP, Paré D. 2008. Theta synchronizes the activity of medial prefrontal neurons during learning. *Learning & Memory*. 15(7):524–531.

Pickart CM, Eddins MJ. 2004. Ubiquitin: structures, functions, mechanisms. *Biochimica et Biophysica Acta (BBA)-Molecular Cell Research*. 1695(1–3):55–72.

Pilon M, Zadra A, Joncas S, Montplaisir J. 2006. Hypersynchronous delta waves and somnambulism: brain topography and effect of sleep deprivation. *Sleep*. 29(1):77–84.

Qi H, Rand MD, Wu X, Sestan N, Wang W, Rakic P, Xu T, Artavanis-Tsakonas S. 1999. Processing of the notch ligand delta by the metalloprotease Kuzbanian. *Science*. 283(5398):91–94.

Risher WC, Ustunkaya T, Alvarado JS, Eroglu C. 2014. Rapid Golgi analysis method for efficient and unbiased classification of dendritic spines. *PloS One*. 9(9):e107591.

Roybon L, Mastracci TL, Ribeiro D, Sussel L, Brundin P, Li JY. 2010. GABAergic differentiation induced by Mash1 is compromised by the bHLH proteins Neurogenin2, NeuroD1, and NeuroD2. *Cerebral Cortex*. 20(5):1234–1244.

Ruan CS, Wang SF, Shen YJ, Guo Y, Yang CR, Zhou FH, Tan LT, Zhou L, Liu JJ, Wang WY, et al. 2014. Deletion of TRIM32 protects mice from anxiety-and depression-like behaviors under mild stress. *European Journal of Neuroscience*. 40(4): 2680–2690.

Salama-Cohen P, Arévalo MÁ, Grantyn R, Rodríguez-Tébar A. 2006. Notch and NGF/p75NTR control dendrite morphology and the balance of excitatory/inhibitory synaptic input to hippocampal neurones through Neurogenin 3. *Journal of Neurochemistry*. 97(5):1269–1278.

Salama-Cohen P, Arévalo MÁ, Meier J, Grantyn R, Rodríguez-Tébar A. 2005. NGF controls dendrite development in hippocampal neurons by binding to p75NTR and modulating the cellular targets of notch. *Molecular Biology of the Cell*. 16(1):339–347.

Schmitt U, Tanimoto N, Seeliger M, Schaeffel F, Leube R. 2009. Detection of behavioral alterations and learning deficits in mice lacking synaptophysin. *Neuroscience*. 162(2): 234–243.

Šestan N, Artavanis-Tsakonas S, Rakic P. 1999. Contact-dependent inhibition of cortical neurite growth mediated by notch signaling. *Science*. 286(5440):741–746.

Sherwood CC, Subiaul F, Zawidzki TW. 2008. A natural history of the human mind: tracing evolutionary changes in brain and cognition. *Journal of Anatomy*. 212(4):426–454.

Snyder JS, Soumier A, Brewer M, Pickel J, Cameron HA. 2011. Adult hippocampal neurogenesis buffers stress responses and depressive behaviour. *Nature*. 476(7361):458.

van der Zee EA. 2015. Synapses, spines and kinases in mammalian learning and memory, and the impact of aging. *Neuroscience & Biobehavioral Reviews*. 50:77–85.

Wang B, Wu Q, Lei L, Sun H, Ntim M, Zhang X, Wang Y, Zhang Y, Ge B, Wu X, et al. 2019. Long-term social isolation inhibits autophagy activation, induces postsynaptic dysfunctions and impairs spatial memory. *Experimental Neurology*. 311:213–224.

Wu Y, Liu Y, Levine EM, Rao MS. 2003. Hes1 but not Hes5 regulates an astrocyte versus oligodendrocyte fate choice in glial restricted precursors. *Developmental Dynamics: An Official Publication of the American Association of Anatomists*. 226(4):675–689.

Xu L, Qiu X, Wang S, Wang Q, Zhao XL. 2019. NMDA receptor antagonist MK801 protects against 1-Bromopropane-induced cognitive dysfunction. *Neuroscience Bulletin*. 35: 347–361.

Yan J, Pan Y, Zheng X, Zhu C, Zhang Y, Shi G, Yao L, Chen Y, Xu N. 2019. Comparative study of ROCK1 and ROCK2 in hippocampal spine formation and synaptic function. *Neuroscience Bulletin*. 35:649–660.

Yizhar O, Fenno LE, Prigge M, Schneider F, Davidson TJ, O'shea DJ, Sohal VS, Goshen I, Finkelstein J, Paz JT, et al. 2011. Neocortical excitation/inhibition balance in information processing and social dysfunction. *Nature*. 477(7363):171.

Yokota T, Mishra M, Akatsu H, Tani Y, Miyauchi T, Yamamoto T, Kosaka K, Nagai Y, Sawada T, Heese K. 2006. Brain site-specific gene expression analysis in Alzheimer's disease patients. *European Journal of Clinical Investigation*. 36(11):820–830.

Yudofsky SC, Hales RE, London AS, Karel MJ, Ogland-Hand S, Solms M, NewYork O, Solms BM, Chan CH, Luo JS, et al. 2002. The American Psychiatric Publishing textbook of neuropsychiatry and clinical neurosciences. *British Journal of Psychiatry*. 181:549–550.

Zhang HM, Liu P, Jiang C, Jin XQ, Liu RN, Li SQ, Zhao Y. 2018. Notch signaling inhibitor DAPT provides protection against acute craniocerebral injury. *PLoS One*. 13(2):e0193037.

Zhu JW, Zou MM, Li YF, Chen WJ, Liu JC, Chen H, Fang LP, Zhang Y, Wang ZT, Chen JB, et al. 2019. Absence of TRIM32 leads to reduced GABAergic interneuron generation and autism-like behaviors in mice via suppressing mTOR signaling. *Cerebral Cortex*. 00:1–19.